



Rapid Synthesis of Gold Nanoparticles with Ginger Waste using Microwave Irradiation

G. BHAGAVANTH REDDY¹, B. RAJKUMAR², K. GIRIJA MANGATAYARU¹ and T.V.D. PRASAD RAO^{2,*}

¹Department of Chemistry, Palamuru University, Mahabub Nagar-509001, India

²Department of Chemistry, Osmania University, Hyderabad-500007, India

*Corresponding author: E-mail: thyp123@gmail.com

Received: 25 October 2019;

Accepted: 6 December 2019;

Published online: 30 December 2019;

AJC-19745

In the present investigation, synthesis of gold nanoparticles (AuNPs) was carried out with microwave irradiation of HAuCl_4 and the extract of ginger waste. Synthesized AuNPs were characterized by various techniques including UV-visible spectroscopy (UV-vis), Fourier transform infrared spectroscopy (FTIR), X-ray powder diffraction (XRD), dynamic light scattering (DLS) and transmission electron microscopy (TEM). The TEM images revealed that the nanoparticles were spherical in shape and the average particle size of the AuNPs was found to be approximately 6 ± 2 nm. The stability of gold nanoparticles was analyzed by zeta potential measurements. A negative zeta potential value of -18.4 mV indicates the stability of the AuNPs. Further, gold nanoparticles exhibited the excellent catalytic activity in reducing 4-nitrophenol to 4-aminophenol in the presence of NaBH_4 (reducing agent), and it was found to depend on the amount of AuNPs and temperature. Gold nanoparticles did not show any significant antibacterial activity against the pathogenic bacteria studied.

Keywords: Gold nanoparticles, Green synthesis, Ginger waste, Catalytic activity, Antibacterial activity.

INTRODUCTION

The discharge of industrial wastes or effluents from pharmaceutical, textile and other industries are the prime reasons for ecological contamination. For this reason, the control of industrial effluents is a vital task, which help the creating a hygienic and inoffensive environment [1-3]. Main chemicals like 4-nitrophenol and nitrophenol derivatives are considered to be by products of many pharmaceutical reactions. These chemicals are environmentally carcinogenic materials because of their repressive nature, high solubility in water and have a tendency to induce the accumulation in deep soil [4].

4-Nitrophenol may cause some harmful effects on human physiology like confusion, eye irritation, cognitive state and cyanosis. By considering the above stated impacts, reduction of nitrophenols are one of the important task in the present research field. The conventional procedures, including absorption, chemical coagulation and reverse osmosis cannot be effective and enough for the reduction of nitrophenols (toxic) to non-toxic products (amino phenols) [5-7]. Therefore, developing a new method is of great interest for the reduction of nitro

phenols. Nanotechnology has been extended to the reduction of nitrophenols in the recent years, due to high surface area of various nanoparticles shows a greater reactivity.

Among the several noble metal nanoparticles, gold nanoparticle has become the focus of intensive research due to surface plasmon resonance properties which are strongly related to their shape, size and interparticle distance [8]. Further, AuNPs are of great attention due to their application in biological and chemical sensing, medical, imaging, and electrochemistry [9]. Conventionally, various methods have been employed for the synthesis of AuNPs such as chemical reduction, photochemical reduction, radiolysis and laser ablation [10]. These methods are using hazardous and environmentally lethal chemicals, which have potential environmental and biological risk [11-15]. Presently, use of natural materials for the synthesis of AuNPs has become an alternative solution. Several studies [9,12,16-18] have been reported for the synthesis of AuNPs by using different plants and their parts. Specific plant and plant based wastes have been successfully used for the synthesis of AuNPs and the plant based materials are capable of producing a wide variety of stable AuNPs, in which plant phytochemicals

such as terpenoids, polyphenols and biomolecules such as polysaccharides, amino acids, vitamins, proteins, act as both reducing and capping agents [19-23].

Among the several plants, ginger plant (*Zingiber officinale*) is flowering plant belongs to Zingiberaceae family, originated in Southeast Asia and widely used as a spice and effective folk medicine. The roots of plants are easily available, inexpensive, non-toxic and have a potential application as a food additive. The cultivation of ginger in India is very high and contributes 34 % of total world production. Chemically, ginger mainly consists of phenolic compounds including shogaols, gengerdiones, paradols, gingerols, *etc.* Ginger is one of the effective bioactive components, showing many nutraceutical activities, including antioxidant activity, thermoregulatory effect, gastro protective effect and anti-inflammatory effect [24,25].

In the present study, aqueous extract of ginger waste was used for the synthesis of gold nanoparticles (AuNPs). Ginger waste act as both reducing and stabilizing agent. The AuNPs have been characterized by standard spectroscopic methods. These AuNPs were also studied for their applications as a catalyst in the reduction of 4-nitrophenol in the presence of NaBH_4 in water medium using UV-Vis spectrometry. The antibacterial activity was also carried out against six pathogenic bacteria.

EXPERIMENTAL

Chloroauric acid (HAuCl_4) was purchased from Sigma-Aldrich (India). All other chemicals were of analytical grade purchased from S.D. Fine chemicals. Ginger waste was collected from a waste disposal from local market yard of Hyderabad city.

Preparation of ginger waste extract solution: A ginger waste was washed with distilled water and dried by placing them under sunlight for one week. Then, ginger waste (2 g) were crushed and mixed with 50 mL distilled water and centrifuged at 400 rpm. The mixture was subjected to microwave irradiation for 50 s at 600 W power. The resulting mixture was filtered with Whatman filter paper to get the clear extract.

Synthesis of gold nanoparticles (AuNPs): For a typical synthesis, 5 mL of extract is added to 3 mL of freshly prepared 1 mM solution of HAuCl_4 . The mixture was allowed to boil by microwave rapid heating. Appearance of red colour in the reaction mixture indicates the formation of AuNPs. After this, the coloured solution of AuNPs was centrifuged and AuNPs were redispersed to remove any unreacted ions and molecules from the product.

Characterization: The optical properties of AuNPs were analyzed by UV-Visible spectrometer (Model: Shimadzu UV-Vis 3600). FTIR analysis was carried out (IR Affinity-1), while XRD patterns were obtained using Rigaku, Miniflex. The mean diameter and PDI of AuNPs were recorded on a Malvern instrument Ltd., Serial Number: MAL1004428, UK and TEM (JEOL 2000 FX-II TEM).

Catalytic reduction of 4-nitrophenol: 4-Nitrophenol (1.7 mL of 0.2 mM) was mixed with 1 mL of 0.015 M NaBH_4 in the cell for UV-visible analysis. Immediately, a colour changed from light yellow to deep yellow and AuNPs solution

was added to the above mixture. The UV-visible absorption spectra were recorded with a time interval in a scanning range of 200-700nm.

Antibacterial activity: A agar well diffusion assay was performed to study the antibacterial activity of AuNPs. The target pathogenic bacteria (10^7 CFU/mL) *viz.* *Staphylococcus aureus*, *Proteus vulgaris*, *Enterococcus*, *Escherichia coli*, *Bacillus subtilis* and *Klebsiella pneumoniae* were spread on the Muller Hilton agar plates separately. The agar wells were made by using a clean and sterile borer and 100 μL of sample was added inside the well. Plates were incubated at 37 °C for 24 h.

RESULTS AND DISCUSSION

UV-visible analysis: Gold nanoparticles shows a strong absorption band at 515-535 nm due to surface plasmon resonance. The formation of AuNPs was optimized by varying the concentrations of ginger waste, HAuCl_4 and microwave irradiation time. Different concentrations of extracts (0.5-2 %) are mixed with 2 mM HAuCl_4 solution in order to study the effect of ginger waste extract concentration on the formation of AuNPs. It is observed from the UV-visible spectra (Fig. 1) that the formation of AuNPs were increased with an increase in concentration of extract due to reduction of more Au^{3+} ions by biomolecules of extract as AuNPs.

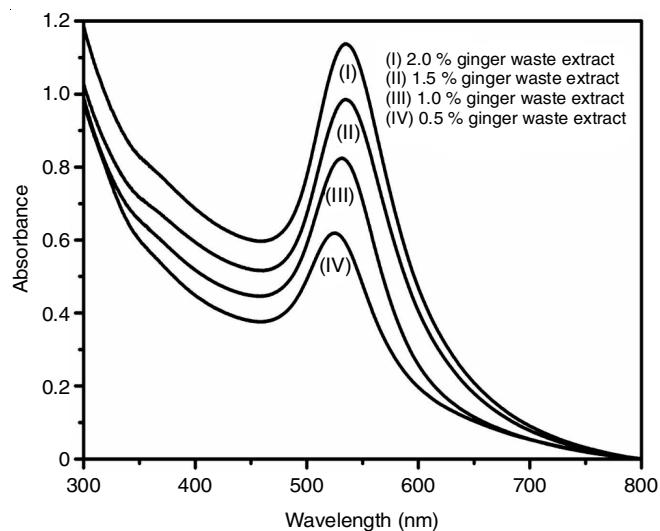


Fig. 1. UV-visible absorption spectra of AuNPs synthesized at different concentrations of ginger waste extract

The UV-visible spectra for AuNPs synthesized by mixing different concentrations of HAuCl_4 (0.5-2.0 mM) with fixed concentration of the extract is shown in Fig. 2. It was observed that the formation of AuNPs increased with increase in the concentration of HAuCl_4 . This may be due to an increase in number Au^{3+} ions, which in turn reduced as AuNPs by biomolecules of extract.

Also, microwave irradiation time has a major effect on the formation of AuNPs (Fig. 3). It was observed from the UV-visible spectra, that the formation of AuNPs increased with an increase in microwave irradiation time. This may be due to increase in thermal energy, which was absorbed by water molecules and in turn increases the rate of reduction of Au^{3+} ions as AuNPs.

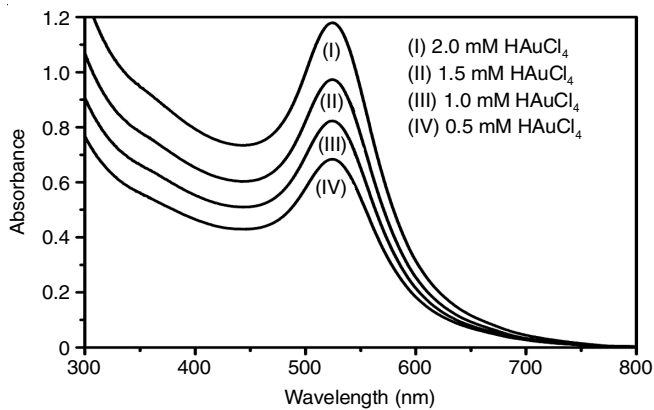


Fig. 2. UV-visible absorption spectra of AuNPs synthesized at different concentrations of HAuCl₄

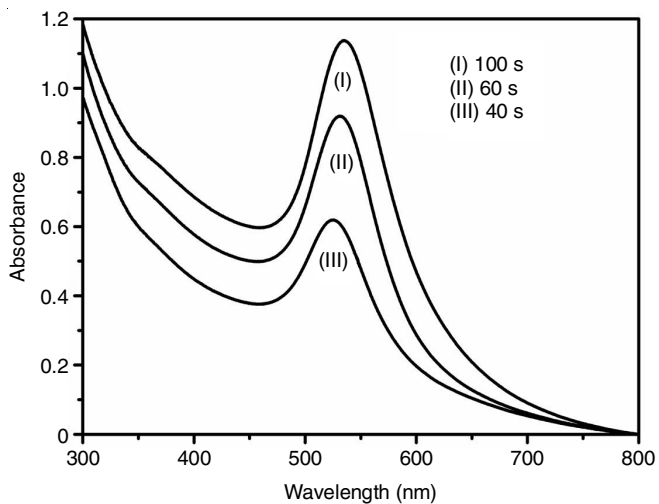


Fig. 3. UV-visible absorption spectra of AuNPs synthesized at different microwave irradiation time

The λ_{max} and full width and half maximum (FWHM) values of AuNPs at various concentrations are presented in Table-1. FWHM and λ_{max} are sensitive to shape and size distribution of AuNPs, stabilizer and refractive index of solution [26]. The λ_{max} of UV-Vis spectra were shifted from 518 to 532 nm (red shift) with the decrease in the concentration of HAuCl₄. The gold nanoparticles were well capped with biomolecules of ginger waste extract and give the red shift. The FWHM values are increasing with the increase in concentration of HAuCl₄ (1.0-2.0 mM) indicates the agglomeration of biomolecules of extract.

TABLE-1 MAXIMUM WAVELENGTH AND FWHM OF VARIOUS CONCENTRATIONS		
Concentration (mM)	λ_{max} (nm)	FWHM
2.0	518	114
1.5	520	107
1.0	528	92
0.5	532	90

FT-IR analysis: The active sites on extract involved in the reduction of Au³⁺ to AuNPs and the formation of AuNPs were investigated by using FT-IR spectroscopy. The FTIR spectrum of ginger waste extract (Fig. 4) shows the major peaks at

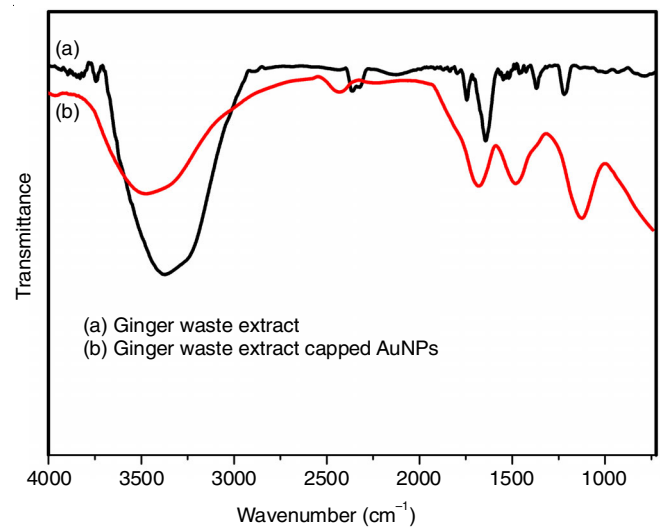


Fig. 4. FTIR spectra of ginger waste extract (a) ginger waste extract capped gold nanoparticles (b)

3374, 1759, 1647 and 1207 cm⁻¹ (curve a). The absorption bands of extract capped AuNPs (curve b) were detected at 3486, 1682, 1478 and 1124 cm⁻¹. The change in the peak positions were observed from 3374 to 3486, 1759 to 1682 and 1674 to 1478 cm⁻¹. These results indicate that hydroxyl groups and carboxyl groups were involved in the synthesis and stabilization of AuNPs.

XRD analysis: The XRD pattern obtained for the AuNPs synthesized with ginger waste extract is shown in Fig. 5. The diffracted intensities were recorded from 10-80°. Four strong Bragg's reflections were observed at 2 θ . The intensities of reflection planes (111), (200), (220) and (311), corresponds to AuNPs structure, are 37.89°, 44.15°, 64.35° and 77.23°, respectively. The average size of AuNPs is calculated by using the Debye-Scherrer formula and found to be 4.5 nm.

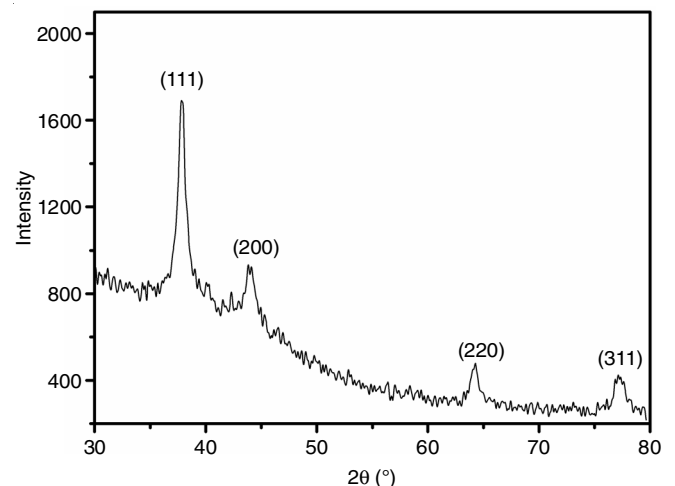


Fig. 5. X-ray diffraction pattern of synthesized AuNPs

Dynamic light scattering (DLS) analysis: The observed particle size of optimized AuNPs was found to be 32.6 nm (Fig. 6a) with 0.392 PDI. The zeta potential (surface potential) value was determined as -18.6 mV (Fig. 6b). The negative value indicates the stability and the size of nanoparticles is less than 100 nm, which indicates that nanoparticles were evaded the

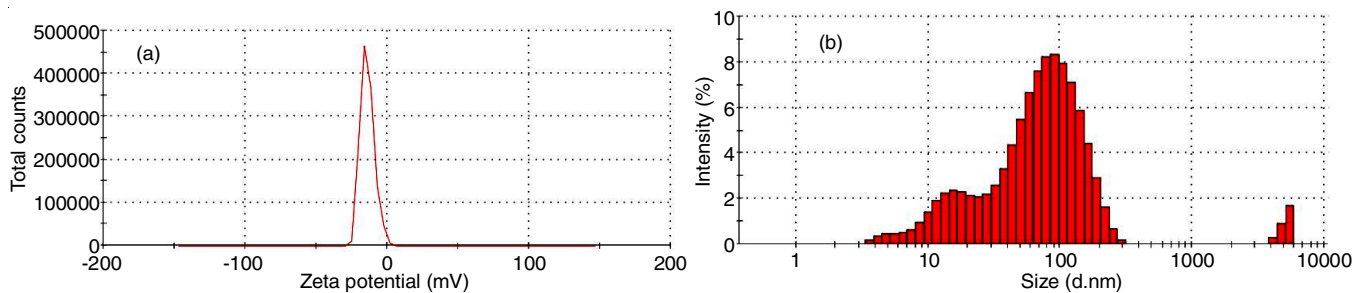


Fig. 6. Zeta potential (a) and size (b) of AuNPs

agglomeration because they are properly capped with biomolecules present in the ginger waste extract. Similar results were reported [27] in the synthesis of gold nanoparticles. The polydispersity index (0.392), which is dimensionless, is less than 0.7, indicated a narrow particle size distribution.

TEM analysis: A TEM analysis of AuNPs (Fig. 7) indicated that the AuNPs were spherical in shape. The size distribution of AuNPs was elucidated from TEM image (Fig. 8) by using the J-software. The average size of AuNPs was determined as 6 ± 2 nm (approximately). This result was consistent with the XRD pattern of the sample.

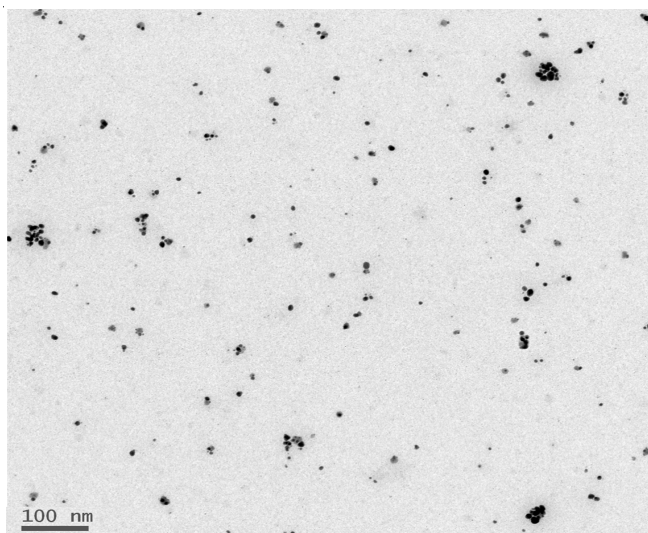


Fig. 7. TEM image of AuNPs

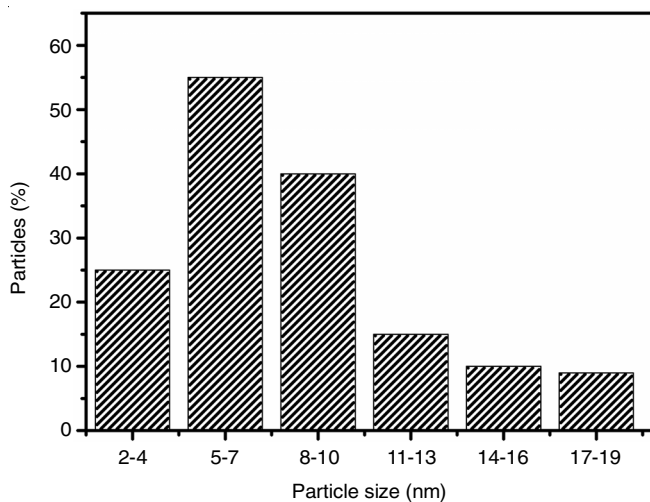
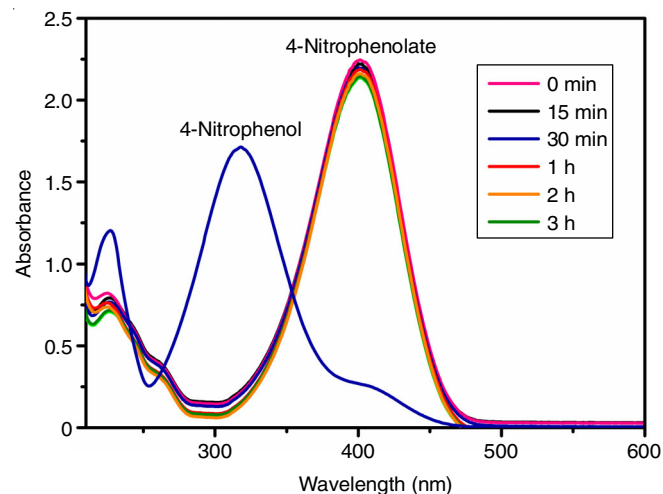


Fig. 8. AuNPs histogram showing the particle size distribution

Catalytic reduction of 4-nitrophenol using AuNPs: In this study, we have taken a model reduction reaction of 4-nitrophenol to 4-aminophenol in the presence of NaBH_4 . The substrates and products of this reaction can be easily monitored by UV-Vis spectrophotometer. The reduction of 4-nitrophenol ($E_{(4\text{-NP}/4\text{-AP})}^0 = -0.76$ V) by NaBH_4 ($E_{(\text{H}_3\text{BO}_3/\text{BH}_4^-)}^0 = -1.33$ V) is thermodynamically feasible but kinetically restricted in the absence of a catalyst. The conversion from 4-nitrophenol to 4-aminophenol occurs *via* an intermediate 4-nitrophenolate ion formation.

4-Nitrophenol shows an absorbance peak at 318 nm and it was red shifts to 400 nm in the presence of NaBH_4 , due to the formation of 4-nitrophenolate ion in the alkaline medium. No reaction was observed when the reaction was conducted without the addition of catalyst. There was no change in the absorbance of peak at 400 nm (Fig. 9). This indicates that NaBH_4 itself was not able to reduce 4-nitrophenolate ion directly.

Fig. 9. UV-visible spectra of 4-nitrophenol and 4-nitrophenol + NaBH_4 without the addition

On addition of AuNPs, there is a rapid decrease in the intensity of the absorption peak at 400 nm, while there is a concomitant appearance of a new peak at 297 nm (Fig. 10) and its intensity increased progressively. This new peak is attributed to the typical absorption of 4-aminophenol. The concentration of NaBH_4 greatly exceeds that of 4-nitrophenol, reduction rate can be assumed to be independent of NaBH_4 concentration. The rate constant (k) was determined from the linear plot of $\ln(A_0/A_t)$ versus reduction time in minutes. This reaction follows pseudo-first-order kinetics with respect to 4-nitrophenol. Our attention was now turned to the dependence of catalytic rate

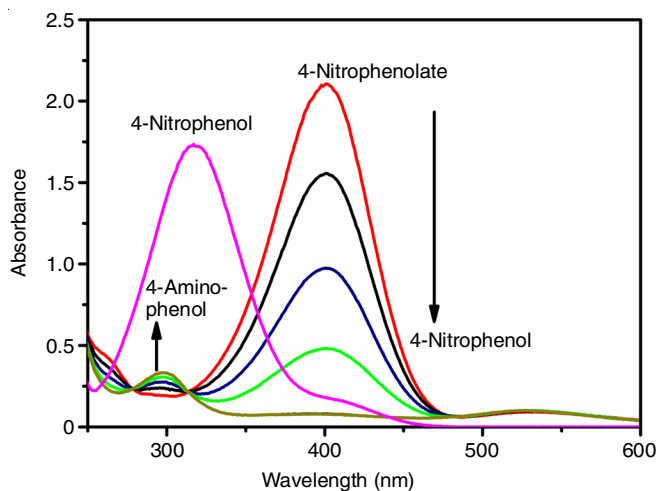


Fig. 10. UV-visible absorption spectra recorded during the reduction of 4-nitrophenol with NaBH_4 catalyzed by AuNPs

on the AuNPs concentration and reaction temperature in the catalytic conversion of 4-nitrophenol to 4-aminophenol.

Gold nanoparticles dosage: The effect of amount of AuNPs on the reduction of 4-nitrophenol to 4-aminophenol was studied using 50-250 μL of AuNPs by keeping other parameters optimized for five catalytic runs. Rate values are plotted against varying amount of catalyst as shown in Fig. 11. As anticipated, k increased with increase in the amount of AuNPs due to an increase in the number of reaction sites.

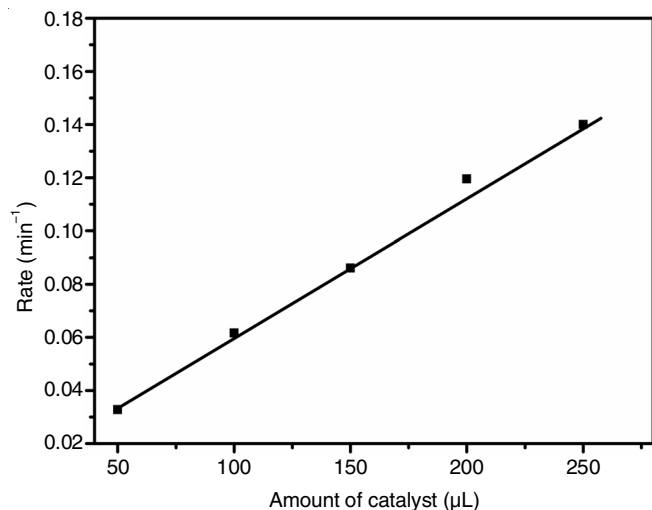


Fig. 11. Effect of amount of AuNPs for the reduction of 4-nitrophenol

The effect of temperature was carried out from 25 to 50 $^{\circ}\text{C}$, for the reduction of 4-nitrophenol to 4-aminophenol. The

activation energy of reaction was obtained from the Arrhenius equation $k = Ae^{-E_a/RT}$, where A is a constant, k is rate constant of the reaction at temperature T (in Kelvin) and R is the universal gas constant. The reaction was studied at six different temperatures (25, 30, 35, 40, 45, 50 $^{\circ}\text{C}$) using AuNPs as catalyst. A plot of $\ln k$ versus $1/T$ showed a linear curve for the reduction of 4-nitrophenol using AuNPs as catalyst. It was observed that the increase in temperature is directly proportional to an increase in the rate of reaction. The activation energy (E_a) was found to be 6.9 kcal/mol.

Antibacterial activity: Antibacterial activity of ginger waste extract capped AuNPs carried out against *Staphylococcus aureus*, *Proteus vulgaris*, *Enterococcus*, *Escherichia coli*, *Bacillus subtilis* and *Klebsiella pneumoniae* using 10, 25, 50, 75 and 100 μL of AuNPs solution. Whereas, small zone of inhibition for *Bacillus subtilis* and *Klebsiella pneumoniae* bacteria at 75 and 100 μL of AuNPs was observed (Table-2). It is concluded that AuNPs did not show any significant antibacterial activity against all the six pathogenic bacteria studied.

Conclusion

A facile, low cost and environmental friendly synthesis of gold nanoparticles (AuNPs) was developed through the reduction of aqueous HAuCl_4 solution using ginger waste extract both as a reducing and stabilizing agent. The synthesized AuNPs were found to be spherical in shape, with a mean diameter of 6 ± 2 nm. The phytochemical analysis suggests that the extract is mainly composed of polyphenols which are liable for rapid reduction of metal salts. A negative zeta potential value of -18.4 mV indicated the stability of AuNPs. The catalytic activity of AuNPs was examined by the reduction reaction of 4-nitrophenol. The detailed kinetic aspects for the catalytic hydrogenation were evaluated by changing the parameters. Further, it was observed that with the increase in AuNPs dose and temperature, total reaction time was decreased and the rate of the reaction was increased. Due to these properties, the synthesized nanoparticles have remarkable applications in biomedical fields. The nanoparticles also showed an excellent catalytic activities towards the reduction of 4-nitrophenol to 4-aminophenol, which helps in the environmental protection. However, as-synthesized gold nanoparticles did not show any antibacterial activity against pathogenic bacteria studied.

CONFLICT OF INTEREST

The authors declare that there is no conflict of interests regarding the publication of this article.

TABLE-2
ZONE OF INHIBITION OF BACTERIAL GROWTH FOR SAMPLES 0.5 mM AND 0.6 mM OF AuNPs

Name of the bacteria	0.5 mM					0.6 mM				
	10 μL	25 μL	50 μL	75 μL	100 μL	10 μL	25 μL	50 μL	75 μL	100 μL
<i>Staphylococcus aureus</i>	0	0	0	0	0	0	0	0	0	0
<i>Proteus vulgaris</i>	0	0	0	0	0	0	0	0	0	0
<i>Enterococcus</i>	0	0	0	0	0	0	0	0	0	0
<i>Escherichia coli</i>	0	0	0	0	0	0	0	0	0	0
<i>Bacillus subtilis</i>	0	0	0.1	0.3	0.5	0	0	0	0.1	0.3
<i>Klebsiella pneumoniae</i>	0	0	0	0	0.1	0	0	0	0	0

REFERENCES

- B.R. Ganapuram, M. Alle, R. Dadigala, A. Dasari, V. Maragoni and V. Guttena, *Int. Nano Lett.*, **5**, 215 (2015); <https://doi.org/10.1007/s40089-015-0158-3>.
- S. Francis, S. Joseph, E.P. Koshy and B. Mathew, *Environ. Sci. Pollut. Res.*, **24**, 17347 (2017); <https://doi.org/10.1007/s11356-017-9329-2>.
- B. Khodadadi, M. Bordbar and M. Nasrollahzadeh, *J. Colloid Interface Sci.*, **490**, 1 (2017); <https://doi.org/10.1016/j.jcis.2016.11.032>.
- S.K. Srivastava, R. Yamada, C. Ogino and A. Kondo, *Nanoscale Res. Lett.*, **8**, 70 (2013); <https://doi.org/10.1186/1556-276X-8-70>.
- J. Zhang, G. Chen, D. Guay, M. Chaker and D. Ma, *Nanoscale*, **6**, 2125 (2014); <https://doi.org/10.1039/C3NR04715F>.
- M. Demirelli, E. Karaoglu, A. Baykal, H. Sözeri, E. Uysal and O. Duygulu, *J. Inorg. Organomet. Polym.*, **23**, 937 (2013); <https://doi.org/10.1007/s10904-013-9870-5>.
- Z. Zhang, J. Zhang, G. Liu, M. Xue, Z. Wang, X. Bu, Q. Wu and X. Zhao, *Korean J. Chem. Eng.*, **34**, 2471 (2017); <https://doi.org/10.1007/s11814-017-0156-4>.
- R.W. Murray, *Chem. Rev.*, **108**, 2688 (2008); <https://doi.org/10.1021/cr068077e>.
- S. Gu, J. Kaiser, G. Marzun, A. Ott, Y. Lu, M. Ballauff, A. Zacccone, S. Barcikowski and P. Wagener, *Catal. Lett.*, **145**, 1105 (2015); <https://doi.org/10.1007/s10562-015-1514-7>.
- T. Tuutijärvi, J. Lu, M. Sillanpää and G. Chen, *J. Hazard. Mater.*, **166**, 1415 (2009); <https://doi.org/10.1016/j.jhazmat.2008.12.069>.
- W. Wang and N. Tao, *Anal. Chem.*, **86**, 2 (2014); <https://doi.org/10.1021/ac403890n>.
- S. Dhar, E.M. Reddy, A. Shiras, V. Pokharkar and B.L.V. Prasad, *Chem. Eur. J.*, **14**, 10244 (2008); <https://doi.org/10.1002/chem.200801093>.
- J.A. Dahl, B.L.S. Maddux and J.E. Hutchison, *Chem. Rev.*, **107**, 2228 (2007); <https://doi.org/10.1021/cr050943k>.
- G.B. Reddy, A. Madhusudhan, D. Ramakrishna, D. Ayodhya, M. Venkatesham and G. Veerabhadram, *J. Nanostruct. Chem.*, **5**, 185 (2015); <https://doi.org/10.1007/s40097-015-0149-y>.
- M. Xiaoyuan, X. Xumin, Y. Xia and Z. Wang, *Foodcont.*, **84**, 232 (2018).
- L. Pethakamsetty, K. Kothapenta, H.R. Nammi, L.K. Ruddaraju, P. Kollu, S.G. Yoon and S.V.N. Pammi, *J. Environ. Sci.*, **55**, 157 (2017); <https://doi.org/10.1016/j.jes.2016.04.027>.
- S. Fazal, A. Jayasree, S. Sasidharan, M. Koyakutty, S.V. Nair and D. Menon, *ACS Appl. Mater. Interfaces*, **6**, 8080 (2014); <https://doi.org/10.1021/am500302t>.
- T.Y. Suman, S.R. Radhika Rajasree, R. Ramkumar, C. Rajthilak and P. Perumal, *Spectrochim. Acta Mol. Biomol. Spectrosc.*, **118**, 11 (2014); <https://doi.org/10.1016/j.saa.2013.08.066>.
- G.B. Reddy, D. Ramakrishna, A. Madhusudhan, D. Ayodhya, M. Venkatesham and G. Veerabhadram, *J. Chin. Chem. Soc.*, **62**, 420 (2015); <https://doi.org/10.1002/jccs.201400513>.
- C. Jayaseelan, R. Ramkumar, A.A. Rahuman and P. Perumal, *Ind. Crops Prod.*, **45**, 423 (2013); <https://doi.org/10.1016/j.indcrop.2012.12.019>.
- M.V. Sujitha and S. Kannan, *Spectrochim. Acta Mol. Biomol. Spectrosc.*, **10**, 215 (2013).
- K. Anand, R.M. Gengan, A. Phulukdaree and A. Chuturgoon, *J. Ind. Eng. Chem.*, **21**, 1105 (2015); <https://doi.org/10.1016/j.jiec.2014.05.021>.
- B.R. Gangapuram, R. Bandi, M. Alle, R. Dadigala, G.M. Kotu and V. Guttena, *J. Mol. Struct.*, **1167**, 305 (2018); <https://doi.org/10.1016/j.molstruc.2018.05.004>.
- R. Ahmad and R. Kumar, *J. Environ. Manage.*, **91**, 1032 (2010); <https://doi.org/10.1016/j.jenvman.2009.12.016>.
- R. Kumar and R. Ahmad, *Desalination*, **265**, 112 (2011); <https://doi.org/10.1016/j.desal.2010.07.040>.
- H. Barani, M. Montazer, T. Toliyat and N. Samadi, *J. Liposome Res.*, **20**, 323 (2010); <https://doi.org/10.3109/08982100903544177>.
- S.V. Patil, H.P. Borase, C.D. Patil and B.K. Salunke, *Appl. Biochem. Biotechnol.*, **167**, 776 (2012); <https://doi.org/10.1007/s12010-012-9710-z>.